Advanced Cusp Field Thruster with a 3D-printed discharge channel - Performance with Iodine and Xenon

IEPC-2019-A-621

Presented at the 36th International Electric Propulsion Conference
University of Vienna, Austria
September 15-20, 2019

Max Vaupel[*], Nils Gerrit Kottke, Alexander Sell, Werner Konrad, Noah Saks, Franz Georg Hey[†]
Airbus, Friedrichshafen, Germany

Martin Schwentenwein
Lithoz GmbH, 1060 Vienna, Austria

Martin Tajmar
Technische Universität Dresden, 01307 Dresden, Germany

and

Peter J. Klar
Justus-Liebig-University Giessen, 35392 Giessen, Germany

Abstract: Small satellite constellations require efficient electric propulsion subsystems to enable the required raising and de-orbiting capabilities. A possible thruster candidate for future constellations is the Advanced Cusp Field Thruster (ACFT) that has been developed over the last years by Airbus in Friedrichshafen. The ACFT has a wide operation range featuring specific impulse (Isp) up to 2000 s, power-to-thrust-ratio (PTTR) between 15 W/mN and 35 W/mN and thrust levels up to 14 mN. The performance of an ACFT with conventionally manufactured boron-nitride (BN) discharge chamber will be discussed comparing iodine and xenon. An additive-manufactured (AM) discharge chamber constructed from alumina (Al_2O_3)has been tested with xenon and the results are compared to those using a BN discharge chamber. Furthermore, we have analysed the electric performance of the ACFT with xenon, monitoring the anode current using a high frequency current probe during ignition and normal operation at various points of operation.

[*]PhD student, Laboratory for Enabling Technologies / JLU Giessen, max.vaupel@airbus.com.
[†]Technical Lead, Laboratory for Enabling Technologies, franz.hey@airbus.com.

Nomenclature

ACFT	=	Advanced Cusp Field Thruster
AM	=	Additive Manufacturing
BN	=	Boron-nitride
HET	=	Hall-Effect Thruster
I_{sp}	=	Specific impulse
LCM	=	Lithography-based Ceramic Manufacturing
MFC	=	Mass flow controller
PTTR	=	Power to thrust ratio

I. Introduction

A new age of satellite design has been ushered in with the foundation of OneWeb in 2015, denoting a transition in the commercial communication satellite business from small numbers of large geostationary satellites towards constellations of hundreds of small satellites in the low earth orbit. One key component for a successful operation of constellations is the propulsion subsystem that is used to perform the orbit raising after the low orbit injection. Electric propulsion offers a significant reduction in propellant mass compared to chemical propulsion but with the drawback of much smaller thrust levels resulting in a longer time to orbit. Since launch costs are one of the driving parameters for a low earth orbit constellation, electric propulsion has been selected for OneWeb as well as the Starlink constellation of SpaceX.

Both constellations are driven by Hall-Effect Thrusters (HET). While OneWeb is operating the HET with xenon as today's common propellant, SpaceX has opted for krypton which is less expensive compared to xenon. Xenon as well as krypton are noble gases that are relatively simple to ionise. Furthermore, they are chemically inert, i.e. there is no risk of contamination of the satellite. The drawback of noble gases is the need for pressurised tanks that contribute significantly to the system mass. An alternative propellant is iodine as it may be stored as a solid at room temperature and sublimates at moderate temperatures, around 100°C. Furthermore, iodine gets vaporised in a molecular state allowing, in principle the formation of heavy ions with nearly twice the mass of xenon.

Besides the utilisation of novel propellants, manufacturing and assembly processes have to be reassessed. Additive Manufacturing (AM) is a unique type of manufacturing process, particularly for ceramic components. The application of AM allows the production of parts and components that are very difficult or even impossible to produce with conventional tooling.

A. Advanced Cusp Field Thruster

The Advanced Cusp Field Thruster (ACFT) has been developed by Airbus Friedrichshafen as a promising new type of electric propulsion system for small satellites. The principle is based on magnetic mirrors, which will reflect charged particles, if their velocity parallel to the magnetic field lines is high enough. Utilisation of multiple magnetic mirrors create so called 'magnetic bottles', yielding a confinement of charged particles. This effect is applied in the ACFT to restrain high energetic electrons in the discharge channel, i.e. in the ionisation area. The magnetic confinement ensures that the electrons transfer their kinetic energy through collisions into ionisation, instead of hitting the anode with high energy. Typical anode potentials are between 200 V and 2000 V. The ion energy, and in a small range also the plasma plume, is defined by the anode potential. Therefore, an adjustment of the specific impulse to meet the needs of the satellite can be performed by tuning the anode voltage. Since no grid or discharge channel erosion occurs in the ACFT, it is not required to specify fixed operation points as commonly done for gridded ion engines or HET.

B. Additive Manufacturing of ceramic parts

Additive manufacturing (AM) represents an emerging production technique with particular strengths for fabricating components in small lot sizes (small-scale series or even customised parts) and components with complex and intricate designs that are difficult or impossible to shape using conventional means. For AM of oxide ceramics it has been demonstrated as feasible to produce parts with mechanical properties at eye-level to conventionally produced components. So-called lithography-based techniques (AM techniques based on the concept of photopolymerisation) show especially high potential in this regard; however, one of the current limitations of this technological approach is the achievable part sizes, which are typically smaller compared to other AM techniques for ceramics.

As mechanical properties and integrity were essential requirements of the application, a lithographic printing technique was chosen for fabricating the discharge channels. The CeraFab system is a dedicated AM system for ceramic materials based on the so-called Lithography-based Ceramic Manufacturing (LCM) technology. It employs the principle of spatially resolved photopolymerisation in a layer-by-layer manner. The materials processed by LCM presented are ceramic suspensions comprising a photopolymerizable monomer mixture filled with ceramic particles. In the case of the presented work the used starting material was photocurable alumina suspension comprising alumina powder, acrylate and methacrylate-based monomers, solvents and process additives such as a photoinitiator and a dye; the concentration of aluminium oxide (Al_2O_3, alumina) particles was at 49 %vol. Alumina exhibits a high thermal stability and due to its low absorption of light in UV and visible range, favourable printing properties in a lithographic additive manufacturing process.

The working principle of the CeraFab printer, illustrated in Fig. 1, combines a rotating vat with static wiper blade to coat layers before each exposure step; this enables the processing of highly viscous materials as it is needed for working with suspensions with high concentrations of solids. The exposure sequence uses a combination of LED and a digital micromirror device (digital light processing concept) so that every layer is cured in a single step which is contrast to curing using a laser, where the whole layer information would have to be scanned.

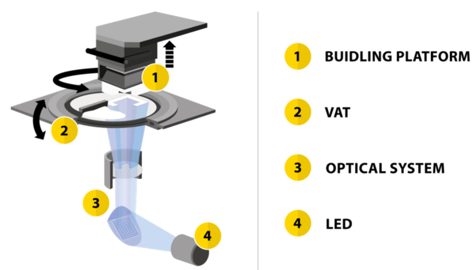

Figure 1: Working principle of a Lithography-based Ceramic Manufacturing system.

The photosensitive ceramic suspension was cured by selective exposure to light of a specific wavelength. Where the light hits the ceramic suspension, the monomers photo-polymerise (harden) into a 3-dimensional network which then acts as a cage for the ceramic filler. After completion of an individual layer, the building platform is elevated along the z-axis by the thickness of a single layer and the whole sequence is then repeated. For the printing of the discharge channels the selected layer thickness was 50 μm.

After layer-by-layer construction using the CeraFab 7500-system, the green parts are cleaned from excess slurry by immersing the part in a solvent able to dissolve the slurry without damaging the cured structure. Subsequent post-processing involves the de-binding of the green part whereby the organic photopolymer matrix is removed through pyrolysis by heating the parts to elevated temperatures. The hereby obtained, so-called white parts are then sintered in a high-temperature oven at 1650°C for 2 hours to produce the final ceramic parts with a homogeneous and isotropic microstructure.

C. Thruster Test Facility

A brief overview of the test facility at Airbus Friedrichshafen is given in this section. The vacuum vessel, which is equipped with plasma diagnostic systems and a highly precise thrust balance, has a volume of 3000 l. The evacuation is performed in three steps, i.e. with a roughing pump with 19 l/s (N_2), a turbo-molecular pump with 2650 l/s (N_2) and two cryopumps with an overall pumping speed of 30,000 l/s. The base pressure, which can be reached without gas ballast is 2e-7 mbar, and with propellant injection of up to 20 sccm xenon no pressure higher than 2e-5 mbar has been measured.

The thrust balance has demonstrated sub-μN resolution and is described in more detail in.[1]

The plasma diagnostic system consists of a patented gridless retarding potential analyser that can be used for Faraday and retarding potential measurements.[1] Furthermore, the first design of an E×B-probe has been tested.

A more comprehensive description of the vacuum facility can be found in.[2]

II. ACFT performance analysis

Small satellite constellations demand a different approach in the development of electric propulsion systems compared to the state-of-the-art. As previously mentioned, alternative propellants are one key factor in reducing the mission impact of the propulsion system further. Moreover, novel manufacturing methods need to be evaluated. Therefore, the ACFT has been tested with xenon and iodine in order to assess the impact if the proppelant on the performance, equipped with a conventional manufactured boron-nitride discharge channel. Furthermore, an ACFT equipped with additive manufactured discharge channel made from alumina (Al_2O_3) compound has been tested.

A. Boron-nitride discharge channel ACFT

Fig. 2 illustrates the operation of two ACFT equipped with BN discharge channels. The one on the lower left is operated with iodine, while the one on the upper right uses xenon as propellant. Both thrusters have been fired with tungsten and LaB6 thermionic emitters as neutralisers. Measurement results presented in this subsection for the ACFT with BN discharge channel have been obtained for both propellants using the same thruster.

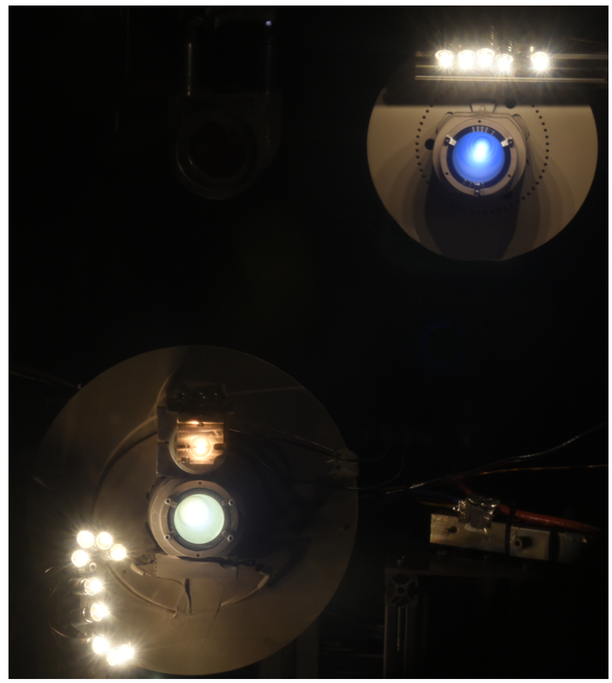

Figure 2: Simultaneous firing of two ACFT with BN discharge channel using iodine and xenon, respectively.

For the xenon tests a Bronkhorst F-201CI-050-ABD-22-V mass flow controller (MFC) with a full range flow of 40 sccm xenon has been used. An exemplary thrust measurement is depicted in Fig. 3. Anode voltage (red line) has been set to the nominal operation point of 600 V. The mass-flow has been set to 4 sccm xenon at seventy seconds. A delay of 4.7 seconds between the command of mass-flow and the ignition of the thruster results from a pipe length of approximately 2 m between MFC and thruster inlet. The thruster was then operated for 354 s with constant anode voltage and mass-flow resulting in an anode power of 138.6 W. Switch-off has been performed by reducing the propellant flow to zero, while the anode voltage has been constant. Thrust has been measured by taking the difference between the thrust before switch off and the measured value at 450 s. Since the thermal expansion of materials results in a shifted centre of gravity, a drift of the apparent thrust during the operation has been observed. Referencing to the thrust shortly after switch-off allows a compensation of this drift, which is small on the relevant time-scale.

The scheme of thrust measurement has been performed for all xenon operation points presented here. Ignition and operation time vary throughout the test. Nevertheless, the ignition scheme demonstrated the simple start-up of the ACFT, which does not require a specific ignition procedure. Therefore, even in the never observed event of a beam-out, a reignition of the thruster would happen after some seconds as long as propellant flow and anode supply are retained.

Fig. 4 illustrates the parameter mapping performed with the ACFT for a wide range of xenon flow rates with various anode voltages. Thrust levels between below 1 mN up to 7.97 mN have been achieved with 300 V anode voltage as can be seen in Fig. 4a. Even though operation at 300 V is feasible, the performance of the ACFT at this potential is inferior compared to the nominal anode voltage operation range of 500 V to 900 V, since specific impulse values range between 470 s to 1060 s. Nevertheless, the 300 V operation features very low PTTR, reaching values as low as 16.3 W/mN. At mass flow rates higher than 6 sccm, a significant performance loss in terms of PTTR and Isp is observed, which is highlighted by a blue circle in Fig. 4b.

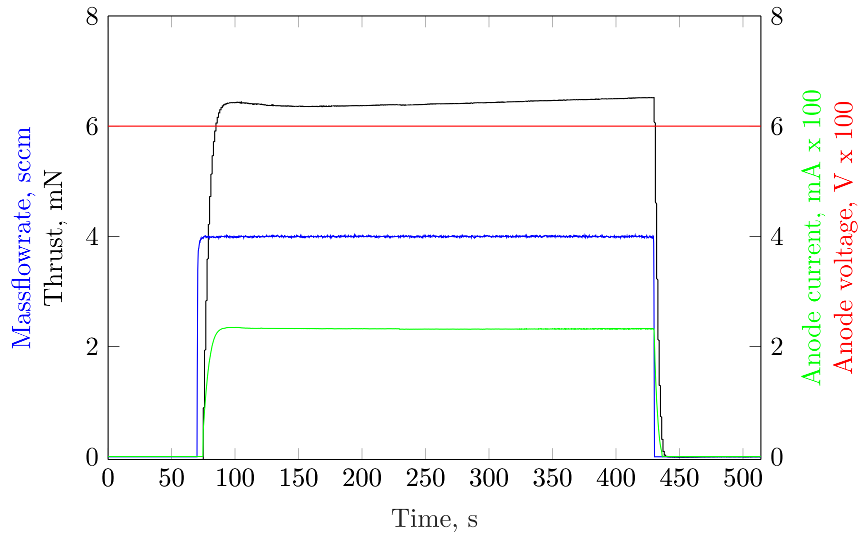

Figure 3: An exemplary thrust measurement performed with the ACFT operated with xenon. Ignition occurs 4.7 seconds after the propellant flow has been commanded, requiring no specific start-up routine.

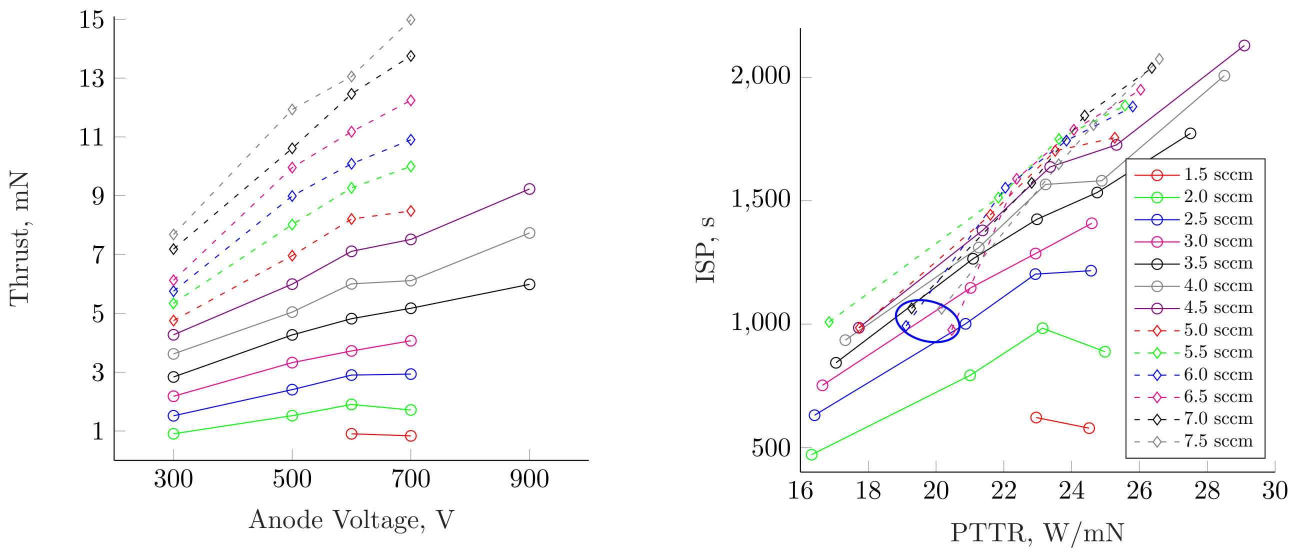

(a) (b)

Figure 4: Parameter maps of the latest configuration of the Advanced Cusp Field Thruster operated with xenon. Fig. 4a is the thrust level map and Fig. 4b illustrates the achieved specific impulse vs PTTR. The blue circle encloses high mass flow rate operation points at 300 V anode potential with particular low performance in terms of PTTR and Isp. The legend in Fig. 4b applies for Fig. 4a as well.

Increasing the anode voltage from 300 V to 500 V has lead to a considerable gain in thrust, ranging from 1.5 mN to 11.9 mN. The PTTR increases to the range from 21 W/mN to 23.6 W/mN with a specific impulse in the range from 792 s to 1648 s. A further increase of the anode voltage from 500 V to 700 V allows ignition and operation of the thruster with even lower mass flow rate, i.e. operation with 1.5 sccm is possible with a measured thrust of 0.83 mN. A maximum thrust of 14.98 mN has been measured with a mass flow rate of 7.5 sccm and an anode power of 398.4 W leading to a PTTR of 26.6 W/mN and a specific impulse of 2074 s.

This remarkable result is limited in the current design of the thruster by thermal restrictions, since the thruster is designed for 300 W operation. Nevertheless, it demonstrates the capabilities of the thruster, if adequate heat removal for higher power operations will be implemented. Limiting the thruster to the design power of approximately 300 W has lead to a thrust of 12.24 mN with 6.5 sccm, a PTTR of 26.1 W/mN, and a specific impulse of 1950 s.

Operation with 900 V anode potential has been observed to be rather unstable with the neutraliser configuration during the here presented test, i.e. high current fluctuations and beam out events occurred on the timescale of several minutes. Nevertheless, three operation points have been stable enough for a reliable measurement showing high specific impulse values above 2000 s, but also very high power-to-thrust-ratios of more than 27.5 W/mN. Since previous tests with different neutraliser configurations have demonstrated stable performance at even higher anode potential, it is assumed that overall performance will increase with a better understanding of the required neutraliser configuration.

Measurements with iodine have been performed without a mass flow controller. The thruster, a small Iodine propellant reservoir, and a feeding pipe form a compact unit, which has been mounted on the thrust balance. Thruster and pipe have been heated to a range of 100 °C to 120 °C, while the tank has been heated to lower values of around 80 °C to 90 °C. Since no fast actuating valve has been implemented in the feedline between thruster and reservoir, thrust measurements have been performed by toggling anode voltage on and off instead of the mass flow. Therefore, thrust values neglect the cold gas thrust.

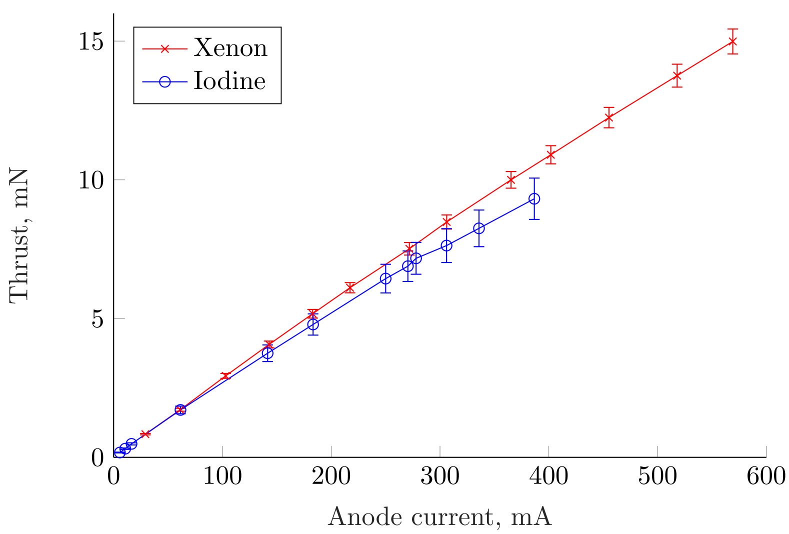

Figure 5: Comparison of the thrust levels achieved with xenon and iodine for various mass flow rates at an anode potential of 700V.

Furthermore, the required heating and thus increased thermal load results in higher thrust measurement uncertainties that have been estimated to 8 %, whereas the xenon thrust measurement uncertainty is only 3 %. Fig. 5 illustrates the comparison of thrust vs. anode current for the BN-ACFT with a constant anode voltage of 700 V. The results are comparable within the limits of accuracy of the measurement, demonstrating iodine suitability as a propellant in terms of power-to-thrust-ratio. Since no mass flow rate has been recorded, the specific impulse can not be evaluated and will be a focus of future research.

B. 3D-printed discharge channel ACFT

Besides the operation of the ACFT with iodine, allowing new applications, additive manufacturing has been used to create an alumina discharge channel as the first proof of principle of 3D-printing for electric propulsion. As mentioned above, additive manufacturing allows the creation of complex parts that are difficult to manufacture with conventional production processes like milling and turning. Even though the discharge channel is produced very efficiently by lathing from a boron-nitride block, this approach does not work for alumina due to its mechanical properties. Two materials have been used, LithaLox350 and D22.

The first test has been performed with the LithaLox 350 discharge channel. During the operation a glowing ring at the position of one cusp was observed. Raising the anode voltage led to arcs from the plasma towards the discharge channel near the bright cusp region. The performance in terms of anode current in relation to mass flow rate has been about 10 % below expectations. During disassembling of the thruster to inspect the discharge channel, the channel broke into two pieces. The line of fracture was coincident with the location of the glowing/ arcing area observed during operation and multiple blackened perforations have been found. Possible explanations for the material failure are mechanical or thermal stress during assembly and operation, respectively, leading to small cracks in the discharge channel.

The LithaLox 350 discharge channel was replaced with the alumina D22 type and the thruster was tested extensively. For this test, only tungsten filaments were used as electron source as electron source. The test results are depicted in Fig. 6 with thrust over anode voltage for various mass flow rates in Fig. 6a and specific impulse over power-to-thrust-ratio in Fig. 6b, respectively. The overall performance of the ACFT with 3D printed alumina discharge channel has been significantly lowered compared to the conventionally manufactured boron-nitride discharge channel. A maximum thrust of 13.5 mN has been achieved with a corresponding specific impulse of 1871 s and a power-to-thrust-ratio of 28 W/mN. The anode voltage at this operation point was set to 700 V with a xenon flow rate of 7.5 sccm.

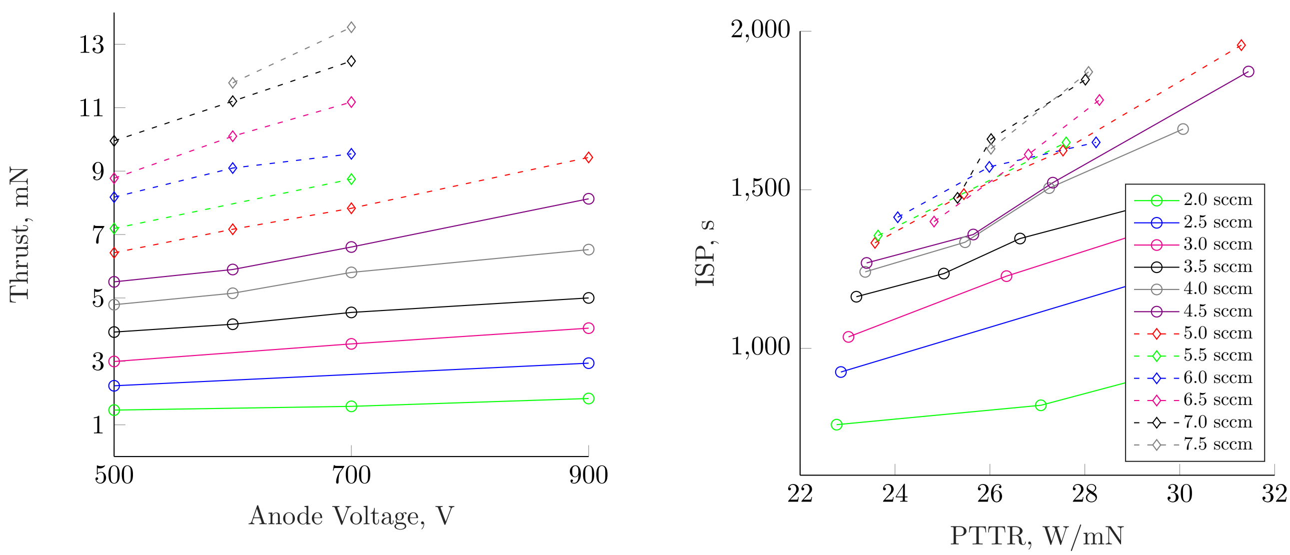

(a)

(b)

Figure 6: Parameter maps of the Advanced Cusp Field Thruster with 3D-printed discharge channel. Fig. 6a is the thrust level map and Fig. 6b illustrates the achieved specific impulse vs PTTR. The legend in Fig. 6b applies for Fig. 6a as well.

Measurements were only conducted at operation points following a successful ignition as illustrated in Fig. 3. Therefore, no operation below 500 V was analysed as no ignition has been triggered. Furthermore, with a xenon flow rate below 2 sccm an ignition was not possible. This leads to a significantly higher minimum thrust with 1.4 mN compared to 0.9 mN with the BN-ACFT. While 7.5 sccm resulted in a peak of 15 mN thrust for the BN-ACFT, the 3D-ACFT was limited to 13.5 mN.

Fig. 7 illustrates the comparison for various xenon flow rates of the BN-ACFT and the 3D-ACFT. The mean deviation was found to be approximately 11.2 %. The reduced performance of the 3D-ACFT has been attributed to the geometrical difference of the discharge channel. Due to the difficulty of reworking sintered alumina with conventional tools, the discharge channel has been produced with a smaller diameter compared to the boron-nitride discharge channel to ensure fitting of the discharge channel in the magnet stack. This reduced diameter leads to a weaker magnetic field inside the discharge channel, reducing the effect of the magnetic bottle and therefore, increases the plasma-wall losses.

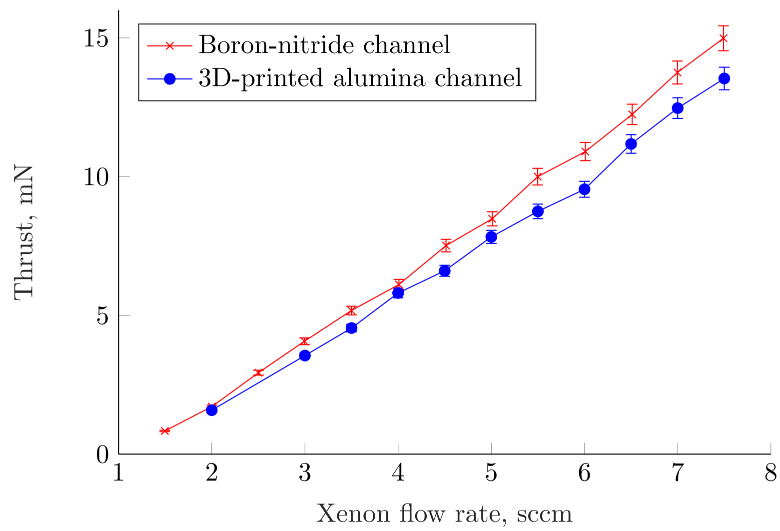

Figure 7: Comparison of the thrust levels achieved with the ACFT with BN and 3D-printed discharge channel for different mass flow rates at an anode potential of 700V.

Accordingly, the result of around 11.2 % reduced performance compared to the BN discharge channel, which has been tailored down to less than 0.1 mm to fit the cusp region, is promising. Taking into account that design and post-processing parameters have not been optimised for the geometry, significant improvements can be expected in the future as curing procedure is the dominant factor regarding the geometrical tolerances.

C. Electrical analysis

Besides the versatility due to the wide operation range of the Advanced Cusp Field thruster, the low anode current noise, i.e. a stable DC-discharge plasma is a notable feature. The anode current has been measured with a high-speed current probe with 80 MHz bandwidth using an oscilloscope with a maximum of 2.5 GS/s. The cable length of the high voltage power supply was approximately 5 m.

Measurements at different operation points have been performed as well as analyses with no mass flow, i.e. no anode current. Furthermore, a measurement with a 4.7 kΩ resistor as the load has been conducted to allow differentiation between thruster induced oscillations and those from the power supply.

Fig. 8 illustrates the measured current spectra. In case of no anode current and with the resistor, the spectra are dominated by peaks at 1550 Hz and higher harmonics, except the second harmonic. Therefore, these features are attributed to the power supply. The highest noise level with thruster operation is also found in the region between 1 kHz and 30 kHz enveloping the power supply peaks. Accordingly, this noise might be attributed to the interdependency of thruster and power supply.

The first thruster anode current eigenfrequency is located between 165 kHz to 195 kHz depending on the anode current, and therefore on the mass flow rate. Harmonics of these frequencies have been observed for all operation points, gaining more intensity with higher anode currents. Above 1 MHz no thruster specific noise has been found.

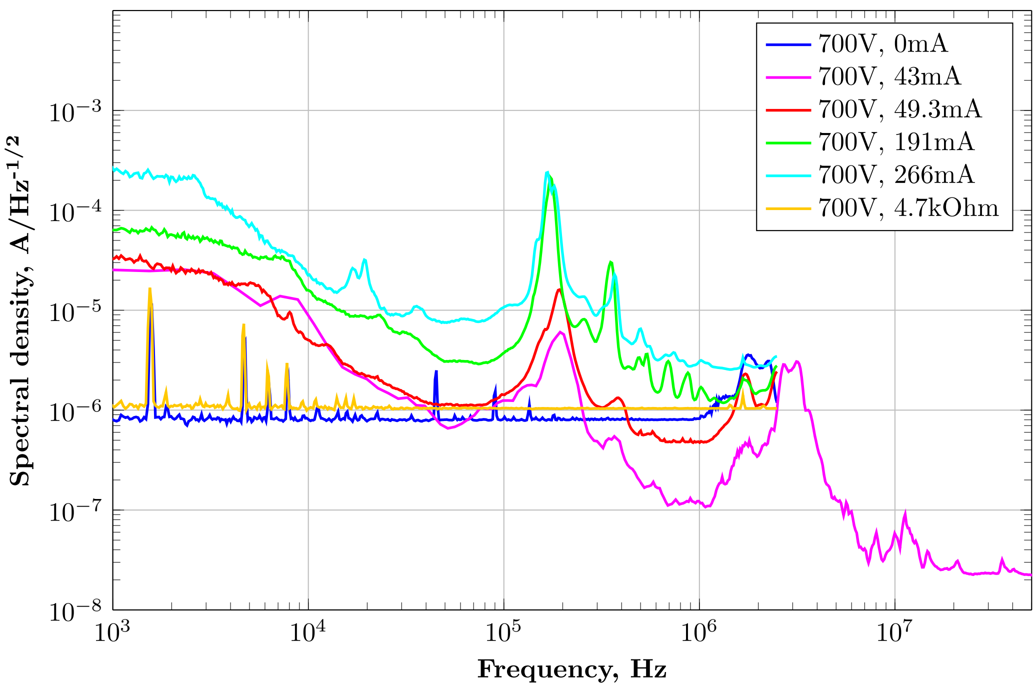

Figure 8: Anode current spectral density for different operation points.

Since iodine discharges tend to be more unstable as a result of the laboratory setup used and the resulting slow flow regulation with frequent current spikes, anode current measurements have been performed with xenon only.

III. Conclusion

Two Advanced Cusp Field Thruster have been extensively tested. The version with a conventionally manufactured boron-nitride discharge channel (BN-ACFT) has been tested with xenon and iodine. With xenon, operation below 1 mN up to 15 mN with specific impulse up to and beyond 2000 s has been demonstrated. Performance with iodine was comparable to xenon in the limits of accuracy of the measurements. Specific impulse has not been evaluated for iodine since no mass flow controller was used for the setup.
Furthermore, a 3D-printed discharge channel has been tested, demonstrating the readiness of additive manufacturing for this kind of application. Reduced performance of about 11.2 % has been achieved compared to the BN-ACFT, which can be attributed to a less form-fitting discharge channel due to minimal optimisation and post-processing of the 3D-printed part.
The anode current has been measured with a high-speed current probe, revealing a low noise floor of the thruster discharge and a oscillation of the discharge between 165 kHz and 195 kHz depending on the anode current.

Acknowledgments

The authors wish to acknowledge the helpful work of participating students of the Laboratory for Enabling Technologies at Airbus Friedrichshafen.
The authors want to thank the German Space Agency DLR for funding through Project No. 50RK1808.

References

[1]Hey, F. G., *Micro Newton Thruster Development*, Springer Vieweg, Berlin, Heidelberg, 2018.

[2]Hey, F. G. et al., "Inter-Laboratory Comparison: Tests of a single thruster in two different facilities, on two different thrust balances," *IEPC-2019-A-656*, 2019.